Electronic Supplementary Information

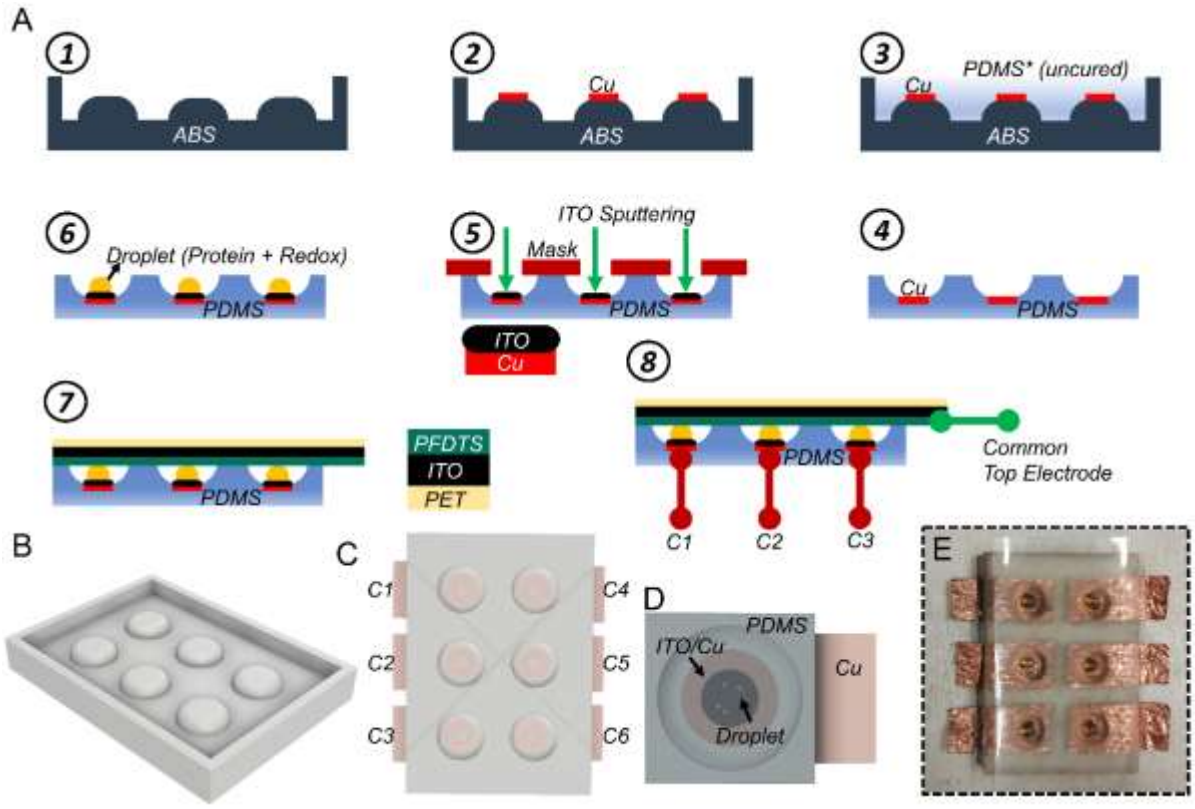

Figure S1: Device fabrication. (A) Step-by-step device fabrication; step ⑧ shows the device terminals; each well in the device serves a capacitor and is connected by a terminal denoted as C1-C6; terminals C4-C6 are at the back in this side-view. **(B)** Model of device mould used for 3D-printing. **(C)** Top view of the bottom-half of the device showing the droplets in the six wells. **(D)** Top view of a single well (pixel). **(E)** Digital photograph of the six-pixel device (average droplet volume ≈3 μL)

Note 1: Optimization of wetting characteristics

The ideal combination of wetting characteristics in the device is a hydrophobic top electrode, a hydrophilic bottom electrode with hydrophobic walls in the well. The wall material is PDMS and is hydrophobic in nature (**Figure S2A**) which aids in maintaining the shape and position of the liquid droplet. The contact angle (CA) on the ITO side of the original ITO/PET sheet (i.e. without a PFDTS coating) is ~91° (**Figure S2B**), which is insufficiently hydrophilic for the bottom electrode and insufficiently hydrophobic for the top electrode. As there is no transparency requirement for the bottom electrode (considering light absorption is through the top-electrode for bio-photocapacitance), the bottom electrode was manufactured by sputtering ITO onto copper foil (see Methods) which not only produced a more hydrophilic ITO surface with a contact angle of ~58° (**Figure S2C**), but also made the electrical contacts from the six bottom electrodes more effective.

Owing to the lack of detailed experimental procedures in the literature for reproducibly constructing a transparent hydrophobic PFDTS layer onto ITO films, five different surface treatment protocols (Phobic 1 to Phobic 5, listed below) were carried out to optimize the hydrophobicity of the ITO/PET top electrode. All five protocols were able to produce a hydrophobic PFDTS-ITO layer **(Figure S2D-H)**. Protocols Phobic 2 and Phobic 5 produced surfaces that were more hydrophobic than the rest, with contact angles of 117° and 116°, respectively, followed by Phobic 1 (CA: ~110°), Phobic 3 (CA: ~108°) and Phobic 4 (CA: ~105°).

Surface Treatment Protocols:

Phobic 1: A solution of PFDTS in ethanol (1:10 (v/v); 100 µL PFDTS + 1000 µL ethanol) and another solution of 1 wt.% acetic acid in propanol (7.65 µL acetic acid + 1000 µL propanol) were mixed together and shaken well. The mixed solution was poured onto a small petri dish and the ITO/PET sheet was immersed in the solution. The ITO/PET sheet was then heated to and maintained at a constant temperature of ~85°C for ~72 minutes. The sheet was left to dry at room temperature for 24 hours and later washed by rinsing with deionized water.

Phobic 2: The two solutions were prepared as in the 'Phobic' protocol. A few drops of the acetic acid:propanol solution was added onto the ITO side of the ITO/PET sheet and left for 10 minutes. The sheet was then heated at ~100°C for 1 hour. Following this, the ITO/PET sheet was immersed in the PFDTS:ethanol solution for 1 hour, after which the sheet was dried at room temperature for 24 hours and then rinsed with deionized water.

Phobic 3: A single solution was prepared by mixing 1000 µL ethanol, 100 µL PFDTS, 1.32 µL acetic acid (1 wt.% acetic acid calculated with respect to PFDTS) and 1000 µL propanol. The ITO/PET sheet was heated to a constant temperature of ~85°C, a few drops of the solution were added onto the ITO and left at the temperature for 30 minutes. The sample was then left to dry at room temperature for 24 hours and later washed by rinsing with deionized water.

Phobic 4: The same steps as in the Phobic 3 protocol were followed, with the exception that small drops of the mixed solution were constantly added onto the ITO surface at ~85°C at ~15 second intervals until the solution was used up. An additional heating period of 30 minutes at ~85°C was included in this protocol before the drying step. The sample was then left to dry at room temperature for 24 hours and later washed by rinsing with deionized water.

Phobic 5: The same steps as in the Phobic 2 protocol were followed, but instead of using 7.65 µL acetic acid, 1.32 µL acetic acid was used (1 wt.% acetic acid calculated based on PFDTS).

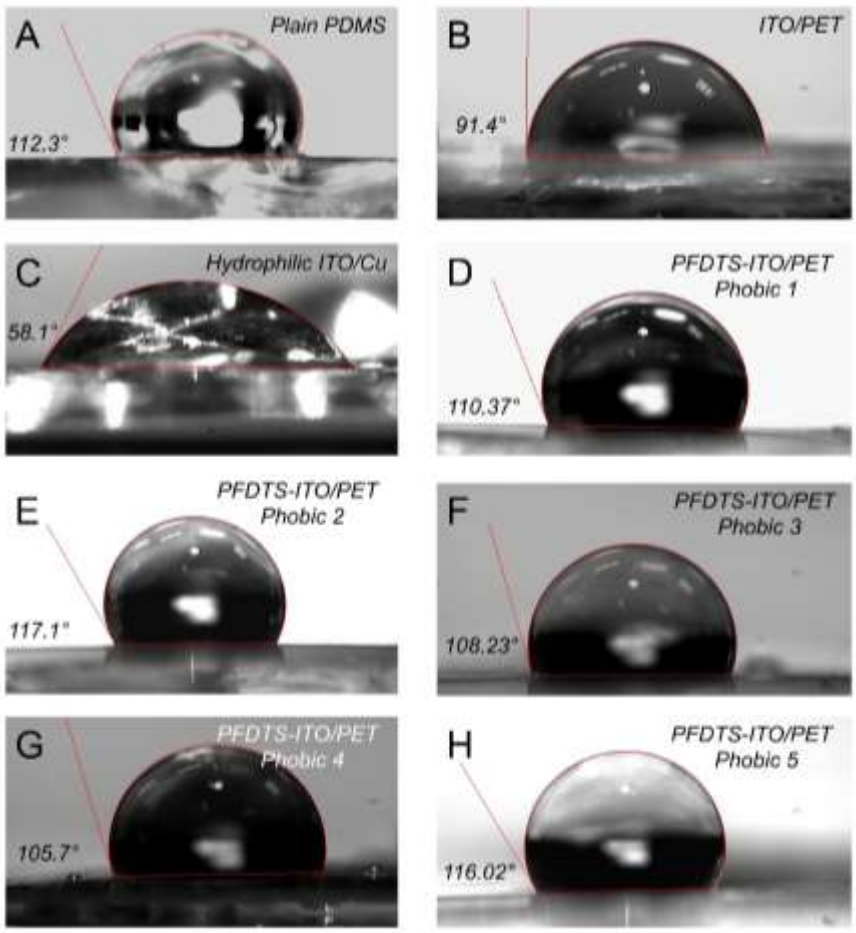

Figure S2: Contact angle measurements. (A) Plain PDMS. **(B)** ITO-coated PET. **(C)** ITO-modified Cu foil. **(D-H)** PFDTS-treated ITO/PET from different surface treatment protocols.

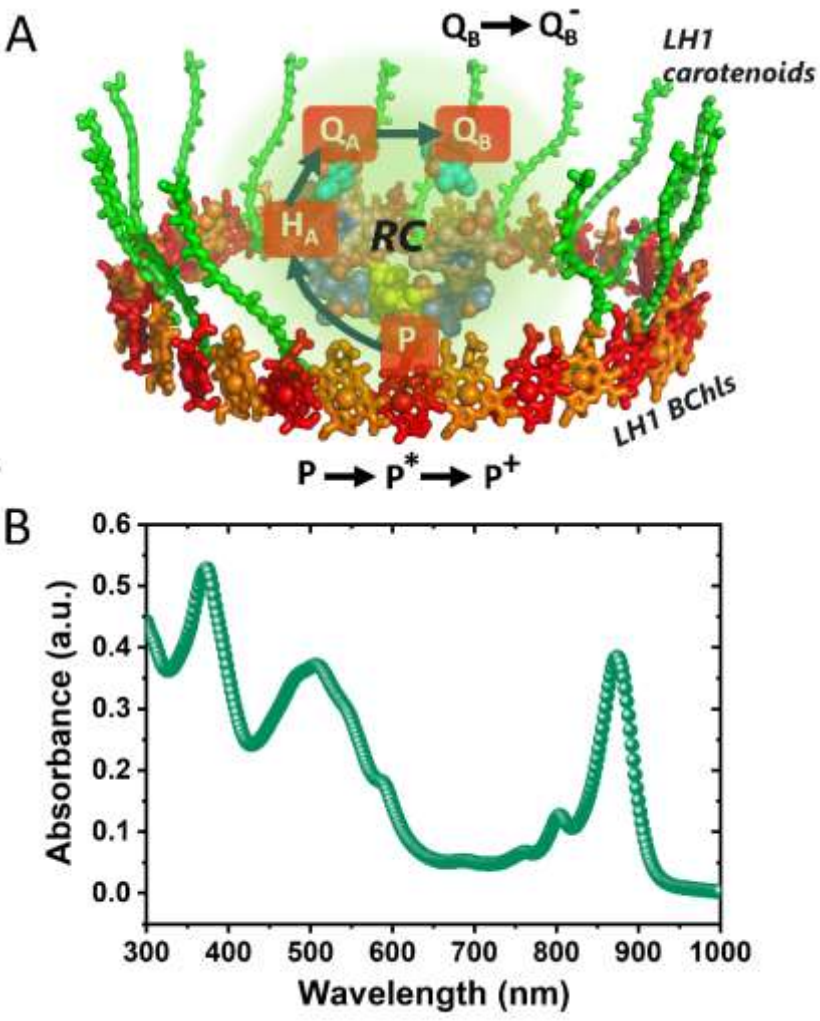

Figure S3: Protein Structure and Photo-absorption Characteristics. (A) Structure of the RC-LH1 protein showing the light harvesting cofactors in the LH1 ring and the electron transport path in the central reaction centre protein (P - excitonically-coupled pair of bacteriochlorophylls (special pair); P* - photoexcited state of the special pair; P^+ - special pair after charge separation, H_A - bacteriopheophytin, Q_A and Q_B - ubiquinone-10). **(B)** Absorbance spectrum of RC-LH1 protein showing a major band at 875 nm attributable to the LH1 domain and minor bands at 805 nm and 760 nm attributable to the central RC.

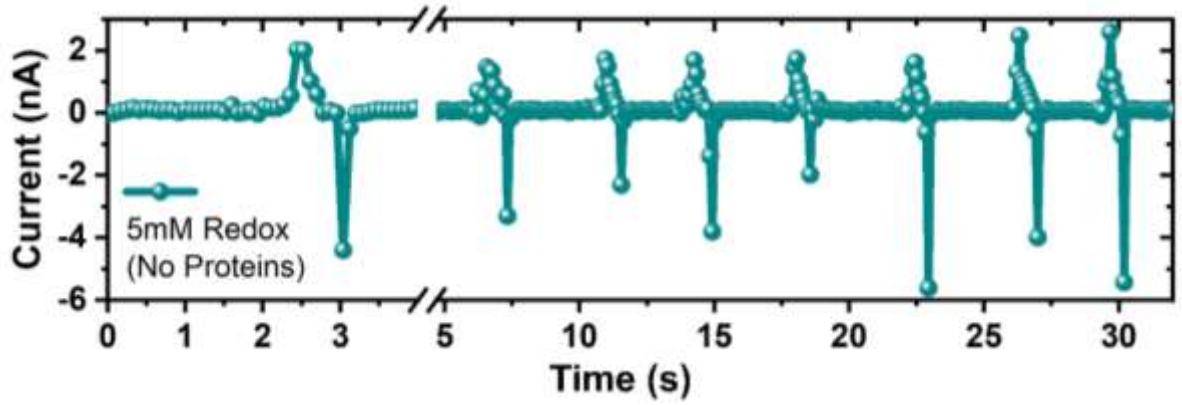

Figure S4: Current response to touch stimuli. Current response to touch stimuli in a device with 5 mM redox electrolyte without RC-LH1 protein.

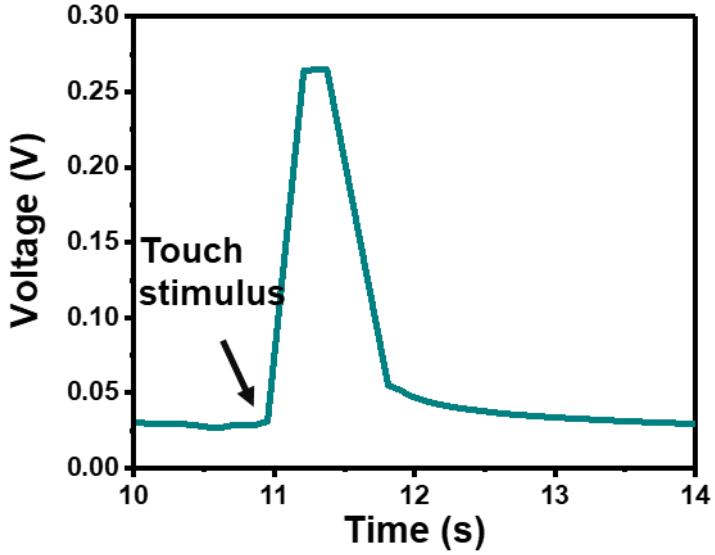

Figure S5: Voltage response to touch stimuli. Voltage response to touch stimuli in a device with 3 µL of RC-LH1 protein but no redox electrolyte.

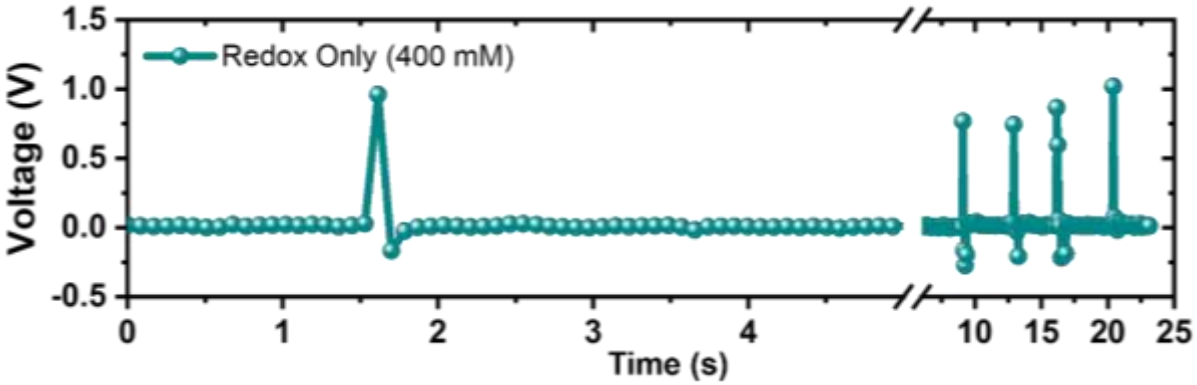

Figure S6: Touch response for a droplet without protein. Voltage response to touch stimuli in a device with 400 mM redox electrolyte without addition of RC-LH1 protein.

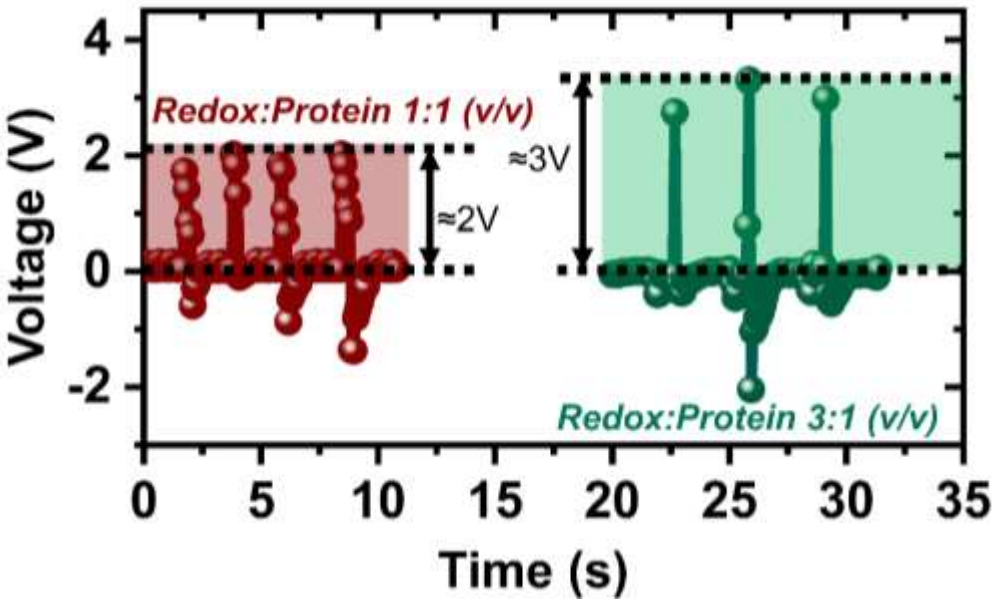

Figure S7: Effect of redox electrolyte-to-protein ratio. Voltage response to touch stimuli in a device with 400 mM redox electrolyte with RC-LH1 protein added in different volume ratios.

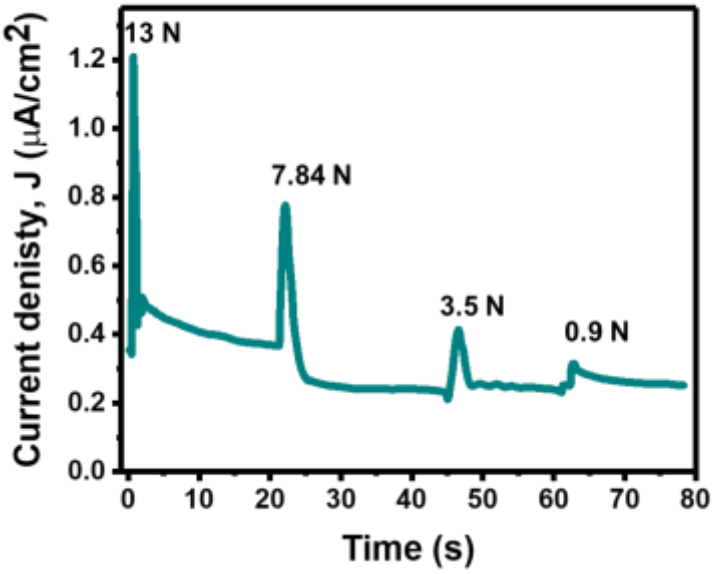

Figure S8: Variation in response to different forces for a single pixel device.

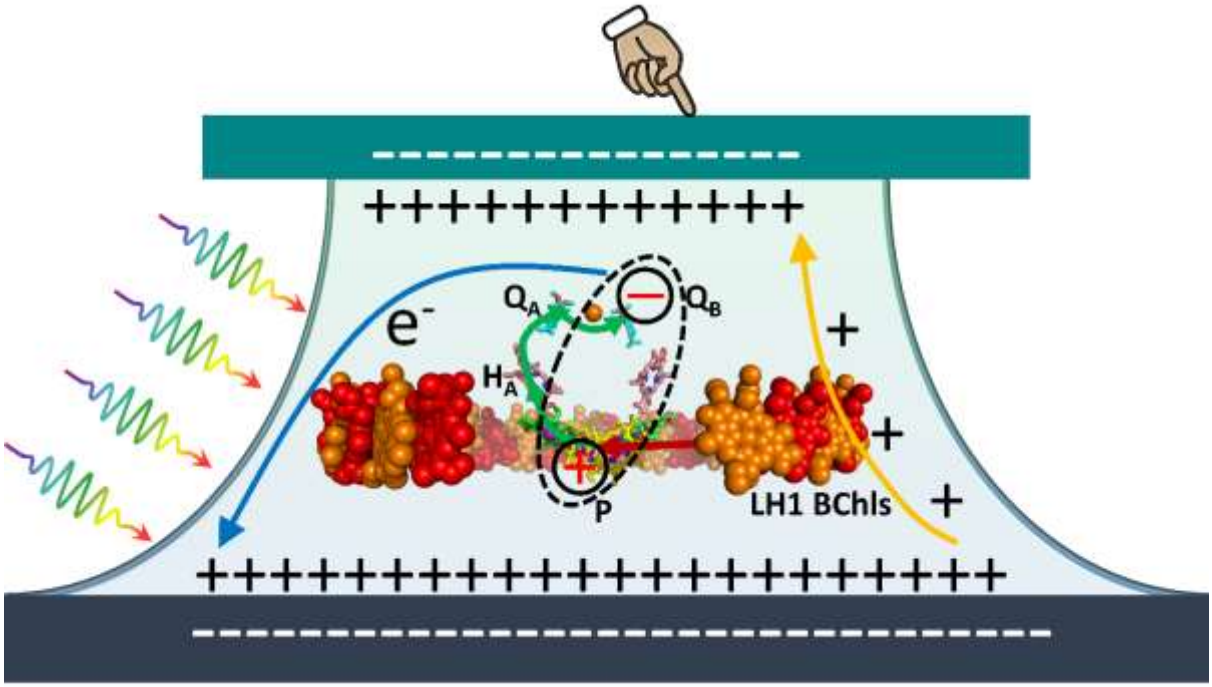

Figure S9: Effect of protein addition on the device charge transfer. Flow of photogenerated electrons from the protein towards the ITO-modified Cu electrode (blue arrow) supplements the flow of positive charge towards the top electrode occurring on touch stimulus (yellow arrow).

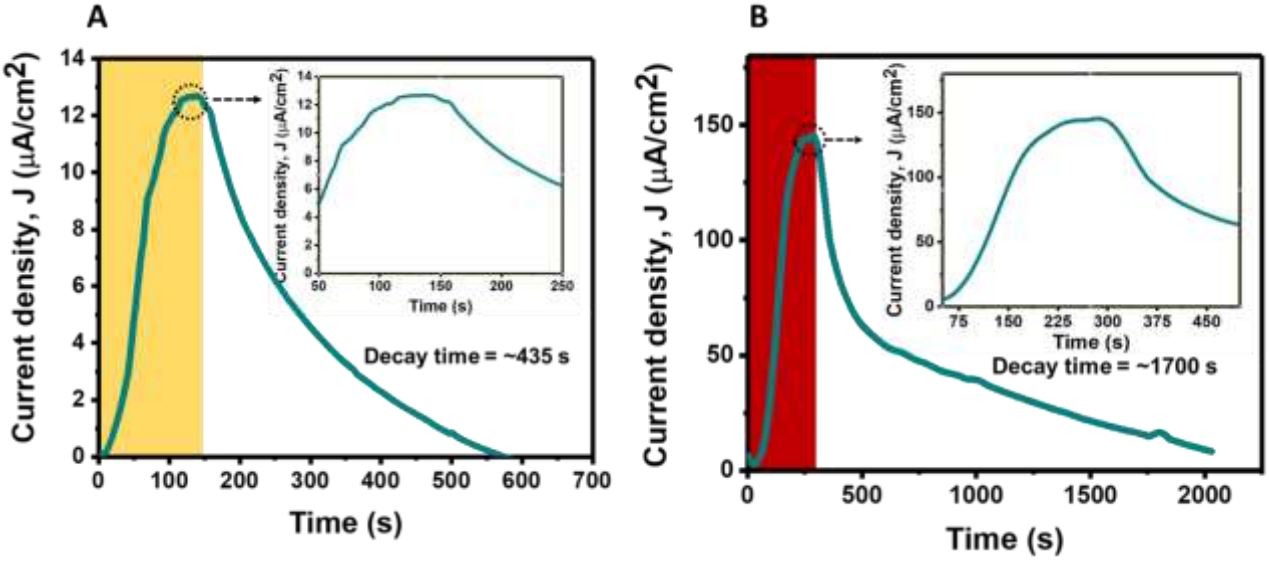

Figure S10: Photocurrent density versus time. (A) response to 30 mW/cm^2 illumination. **(B)** response to 100 mW/cm^2 illumination.

Note 2: Cross-talk Check and Electronic Interface Design

To check for cross-talk between different pixels in the device, a circuit design as shown in **Figure S8** with an external DC power supply (Keithley 2450 Source meter) along with light emitting diodes (green LEDs) was adopted. Each pixel was connected to one LED and thus by pressing a particular pixel, only the specific LED will light up if there is no cross-talk between different pixels (i.e. if stimulating one pixel does not trigger response from any unintended pixel). All the sensors built were checked with this setup and cross-talk was found to be minimal. Simultaneous pressing of various permutations of the pixels in the sensor correctly lit up only the expected LEDs.

Following the cross-talk check, the six-pixel sensor was connected to the electronic interface as shown in the circuit diagram in **Figure S9**. In this setup, the six pixels of the sensors are represented as capacitors C1 to C6. Two ADS1115 16-bit Analog-to-Digital Converters (ADCs) were used to measure analog voltage outputs from the six sensors. Sensors C1, C2, C3, and C4 were connected to one ADC, while sensors C5 and C6 were connected to the other ADC. The two ADCs were connected to an Arduino UNO R3 microcontroller via I²C (Inter-Integrated Circuit), with I²C address of one ADC set to 0x48 and the I²C address of the other ADC set to 0x49. The Arduino UNO R3 microcontroller was connected to a Sparkfun VS053B MP3 Player Shield module with audio clips of the 26 letters of the English alphabet pre-loaded via a microSD card. An audio speaker was connected to the MP3 Player Shield module via a 3.5 mm jack. The setup was programmed to continuously take voltage readings from the six sensors simultaneously via the two ADCs, and play the appropriate alphabet audio clip depending on which sensors were depressed and which sensors were not.

The pixel exhibits a different voltage in “depressed” and “non-depressed” state. To calibrate a pixel, the voltage reading exhibited by the pixel in the “non-depressed” state was recorded, then a stylus was used to depress the pixel and the voltage recorded again. These two voltage readings were then set as the cut-off thresholds for pixel activation/deactivation in the microcontroller program. The process was repeated to calibrate the rest of the pixels. Each pixel had a threshold voltage of 70 mV.

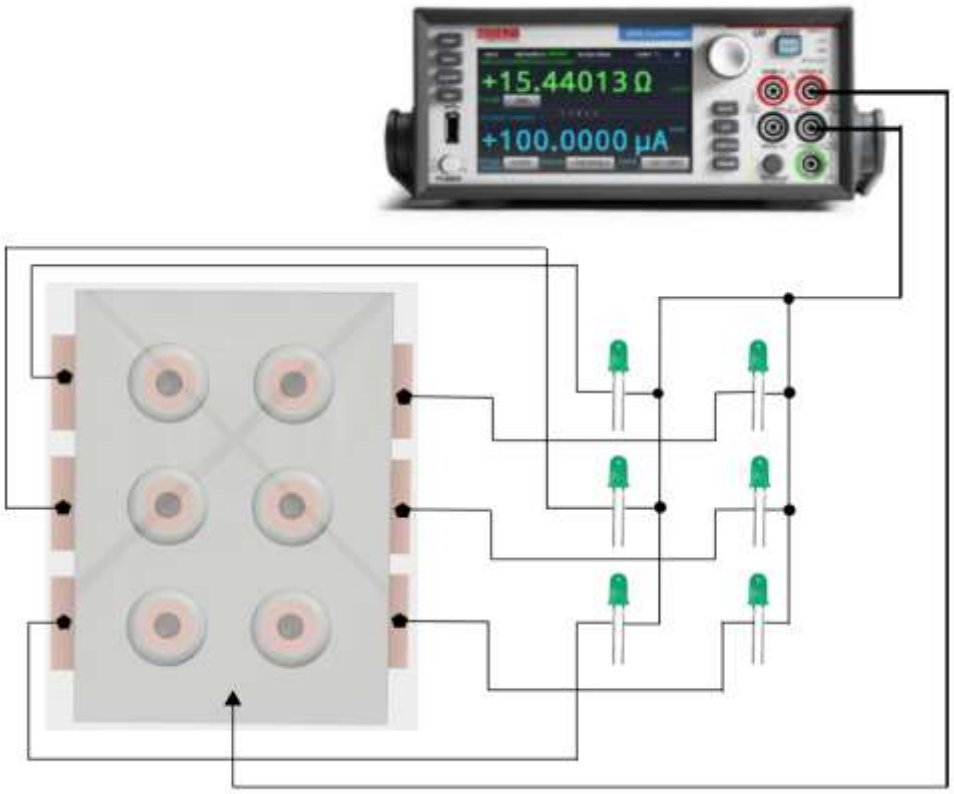

Figure S11: Circuit diagram to check cross-talk. Circuit design adopted to check for cross-talk by simultaneous stimulation of different pixels. Circles (●) denote that the wires are joined and connected to one another; triangles (▲) denote that the wire is connected to the top electrode which is the hydrophobic PFDTS-coated ITO/PET sheet; pentagons (⬟) denote that the wire is connected to the copper foil and thus to the bottom electrode.

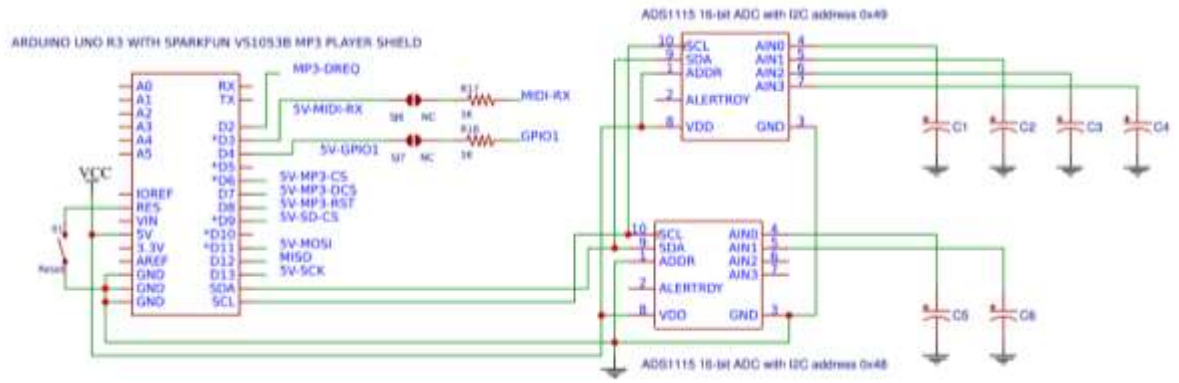

Figure S12: Circuit diagram for the electronic interface

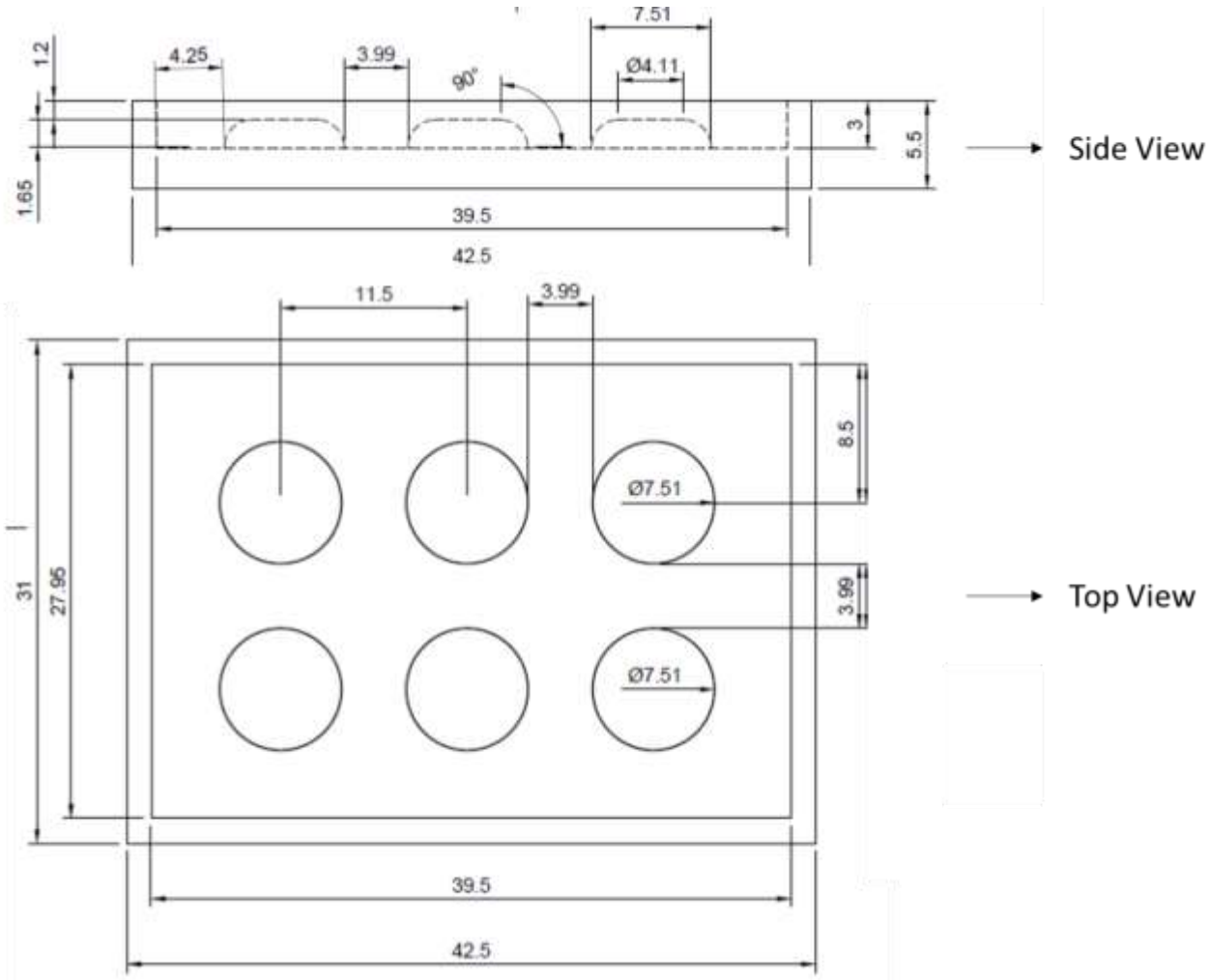

Figure S13: Dimensions of the proposed braille reader in mm.

Type of Braille sensor	Materials	Drawbacks	Year of Publication	Reference
Mechanotransduced Tactile Sensor	Pt cured silicone rubber	• Fluctuations in mechano induced forces are not considered in sensing. • Needs a constant scanning speed. • Expensive fabrication route involving lithography	2017	4
Magnetic tactile sensor	Magnetic Fe nanowires	• Requires a magnetic celia to detect changes in magnetic field and to sense. • Not user friendly	2016	5
Braille Mobile phone (OwnFone)	3D printed metallic Braille keyboard	• Only suitable for making emergency calls • Doesn't provide alphabet reading/learning facilities	2014	6
Tactile Rendering With Shape-Memory-Alloy Pin-Matrix	Nickel titanium (NiTi)	• Material induced complex motion control. • Gives visual representation and hence not applicable for the visually impaired.	2008	7
Phase-Change Micro actuators based Braille display	Paraffins and acetamide	• Depends solely on the thermal response of paraffins and hence the cross-talk is inevitable. • Only an analytical model and no experimental evidence.	2006	8
Braille-Based Chord Gloves	Polyvinylidene fluoride	• Bulky model and cannot press more than two keys at one time • Provides a visual display of sensed letter hence non applicable for visually impaired.	2002	9
Tactile array on the fingertip	lead zirconate titanate	No clear interpretation of the stimuli No threshold mentioned and response to natural touch is uncertain.	2002	10

Table S1: Comparison of similar works especially flexible/wearable devices with our novel touch to audio braille reader.

Force (N)	Rise time (s)	Recovery time (s)
13	0.25	0.58
7.84	0.85	1.4
3.5	1.42	1.5
0.9	1.8	16.5

Table S2: Rise and recovery time with respect to different forces applied onto a single pixel device.

References

1. Yeo, J. C., Liu, Z., Zhang, Z.-Q., Zhang, P., Wang, Z. & Lim, C. T. (2017) Wearable Mechanotransduced Tactile Sensor for Haptic Perception. *Advanced Materials Technologies* **2(6)**:1700006.
2. Alfadhel, A., Khan, M. A., Cardoso, S. & Kosel, J. (2016) Magnetic Tactile Sensor for Braille Reading. *IEEE Sensors Journal* **16**:1-1.
3. https://www.engadget.com/2014/05/19/ownfone-braille-mobile-phone/
4. Velazquez, R., Pissaloux, E. E., Hafez, M. & Szewczyk, J. (2008) Tactile Rendering With Shape-Memory-Alloy Pin-Matrix. *IEEE Transactions on Instrumentation and Measurement* **57(5)**:1051-1057.
5. Green, S. R., Gregory, B. J. & Gupta, N. K. (2006) Dynamic Braille Display Utilizing Phase-Change Microactuators. In *SENSORS, 2006 IEEE*.), pp. 307-310.
6. Myung-Chul, C., Kwang-Hyun, P., Soon-Hyuk, H., Jae Wook, J., Sung Il, L., Hyuckyeol, C. & Hoo-Gon, C. (2002) A pair of Braille-based chord gloves. In *Proceedings. Sixth International Symposium on Wearable Computers*.), pp. 154-155.
7. Summers, I. R. & Chanter, C. M. (2002) A broadband tactile array on the fingertip. *Journal of the Acoustical Society of America* **112(5,Pt1)**:2118-2126.